

Solid-state and Solution Studies of Tungsten(VI) Organoimidoalkoxides†

William Clegg, R. John Errington* and Carl Redshaw

Department of Chemistry, The University of Newcastle upon Tyne, Newcastle upon Tyne, NE1 7RU, UK

The arylimidoalkoxides, $[W(NC_6H_4Me-4)(OR)_4]$ ($R = Me$ or Pr^i) have been shown by X-ray diffraction studies to adopt binuclear, alkoxide-bridged structures in the solid state. The alkoxide bridges are asymmetric [2.072(7) and 2.181(6) Å, $R = Me$; 2.029(4) and 2.243(3) Å, $R = Pr^i$] and coplanar with the terminal arylimido ligands, the longer W–O bonds being *trans* to the short W=N bonds [1.749(8) Å, $R = Me$; 1.738(4) Å, $R = Pr^i$]. Proton NMR studies show that these structures are dynamic in solution, although much less so than their oxo analogues. The bimetallic imidoalkoxide, $[W(NC_6H_4Me-4)(OC_6H_{11})_5Li_2Cl(C_6H_{11}OH)]_2 \cdot C_6H_{11}OH$, obtained from an attempted preparation of $[W(NC_6H_4Me-4)(OC_6H_{11})_4]$, has been shown by a single-crystal X-ray diffraction study to have a dimeric structure analogous to the known rhenium oxoisopropoxide, $[ReO(OPr^i)_5Li_2Cl(thf)]_2 \cdot 2thf$ ($thf =$ tetrahydrofuran). A tungsten(V) imidochloroalkoxide, $[NBu^t_4][W_2(NPh)_2(\mu-Ome)(\mu-Cl)_2Cl_4]$ has also been crystallographically characterised and has a distorted confacial bioctahedral structure in which one of the bridging chlorines is *trans* to both terminal imido groups and the W–W distance is 2.695(1) Å.

The successful use of organoimido ancillary ligands to provide electronic flexibility and steric control in the design of homogeneous alkene metathesis catalysts¹ and the involvement of organoimido species in industrially important catalytic ammoxidation processes² has stimulated synthetic efforts in transition-metal organoimido chemistry during recent years.³ Our interest in oxo and organoimido compounds of the earlier transition metals prompted us to synthesise a range of tungsten alkoxo derivatives in order to investigate and compare their solution properties. We have described the solid-state structures and solution dynamics of oxoalkoxides $[WO(OR)_4]$ in a previous paper,⁴ and we report here our results concerning the analogous organoimidoalkoxides $[W(NR)(OR)_4]$.

Of the previously reported tungsten imidotetraalkoxides $[W(NPh)(OR)_4]$ ($R = Me$ **1**,⁵ Et **2**,⁶ Bu^t **3**^{5,7}), $[W(NMe)(OMe)_4]$ **4**,⁵ and $[W(NBu^t)(OR)_4]$ ($R = Pr^i$ **5**, Bu^t **6**),⁸ only **1** has been crystallographically characterised. This imprecise determination showed a dimeric, centrosymmetric structure similar to those of the *p*-tolylimidochloro⁹ and oxoalkoxo⁴ analogues, $[W(NC_6H_4Me-4)Cl_4]$ **7**, $[WO(OMe)_4]$ **8** and $[WO(OC_6H_{11})_4]$ **9** respectively. In all of these structures, the strongly π -bonding terminal organoimido or oxo ligands are coplanar with the bridging chloro or alkoxo ligands and *trans* to the longer bonds in the asymmetric bridges. This is consistent with the large *trans* influence usually observed for these ligands in d^0 complexes.³ The ¹H NMR spectra reported for **1**, **2** and **4** indicate that dimeric structures persist in solution, whereas for **3**, **5** and **6**, spectra are consistent with mononuclear structures.

Our studies of the oxoalkoxides $[WO(OR)_4]$ have shown that for primary and secondary alkoxides the dimeric structures observed in the solid state are dynamic in solution.⁴ The exact nature of the dynamic processes involved depends on the steric requirements of the alkyl group. When $R = Pr^i$, a monomer/dimer equilibrium exists in solution but for $R = Me$ or Et dissociation into monomers does not occur during intramolecular alkoxide exchange. By comparison, Bradley *et al.*¹⁰ have found the single-line ¹H NMR spectrum of

$[WO(OBu^t)_4]$ to be invariant down to 193 K, showing that the *tert*-butyl group is too bulky to allow dimerisation with a concomitant increase in the co-ordination number of tungsten from five to six.

These dynamic alkoxo complexes provided an opportunity to compare the relative *trans* effects of oxo and organoimido ligands in $[W(E)(OR)_4]$ compounds ($E = O$ or NR). Since we had already structurally characterised the chloro complexes $[W(NC_6H_4Me-4)Cl_4]_2$ ⁹ and $[W(NC_6H_4Me-4)Cl_5]^-$,¹¹ we chose to prepare a range of *p*-tolylimido alkoxides and compare their solid-state and solution properties with those of analogous oxoalkoxides.

Results and Discussion

The arylimidoalkoxides were prepared from $[W(NC_6H_4Me-4)Cl_4]$ by literature methods.^{5–7} Hence, $[W(NC_6H_4Me-4)(OMe)_4]$ **10** was obtained using Bu^tNH₂–MeOH, whereas metathesis with LiOPrⁱ was used for $[W(NC_6H_4Me-4)(OPr^i)_4]$ **11** to avoid the formation of an amine adduct. However, an attempt to obtain $[W(NC_6H_4Me-4)(OC_6H_{11})_4]$ **12** from the chloride **7** and lithium cyclohexoxide resulted in the isolation of the mixed-metal alkoxide $[W(NC_6H_4Me-4)(OC_6H_{11})_5Li_2Cl(C_6H_{11}OH)]_2 \cdot C_6H_{11}OH$ **13**. Single crystals for X-ray diffraction were grown from acetonitrile (**10** and **11**) or by slow diffusion of hexane into a tetrahydrofuran (thf) solution (**13**).

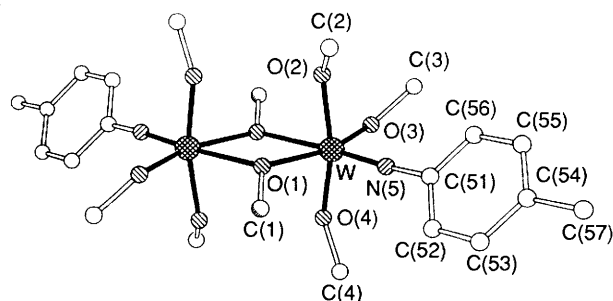


Fig. 1 A view of the molecular structure of complex **10** (Hydrogen atoms are omitted from all structure diagrams for clarity)

† Supplementary data available: see Instructions for Authors, *J. Chem. Soc., Dalton Trans.*, 1992, Issue 1, pp. xx–xxv.

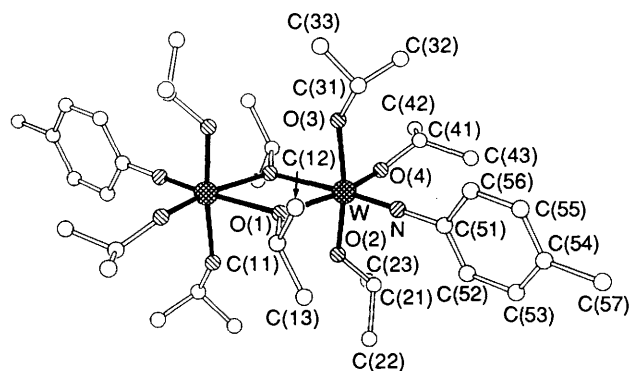


Fig. 2 A view of the molecular structure of complex 11

Table 1 Selected bond lengths (Å) and angles (°) for complex 10

W-O(1)	2.072(7)	W-O(2)	1.922(6)
W-O(3)	1.886(8)	W-O(4)	1.898(6)
W-N(5)	1.749(8)	W-O(1')	2.181(6)
O(1)-C(1)	1.438(15)	O(2)-C(2)	1.383(13)
O(3)-C(3)	1.442(14)	O(4)-C(4)	1.411(14)
N(5)-C(51)	1.394(12)		
O(1')-W-O(2)	82.2(2)	O(1')-W-O(3)	88.9(3)
O(2)-W-O(3)	88.8(3)	O(1')-W-O(4)	83.7(3)
O(2)-W-O(4)	165.8(3)	O(3)-W-O(4)	93.0(3)
O(1')-W-N(5)	168.2(3)	O(2)-W-N(5)	95.9(3)
O(3)-W-N(5)	102.7(4)	O(4)-W-N(5)	97.5(3)
O(1')-W-O(1)	71.5(3)	O(2)-W-O(1)	85.2(3)
O(3)-W-O(1)	160.1(3)	O(4)-W-O(1)	88.4(3)
N(5)-W-O(1)	96.8(3)	W'-O(1)-C(1)	120.1(7)
W-O(1)-W'	108.5(3)	C(1)-O(1)-W	125.1(7)
W-O(2)-C(2)	130.1(6)	W-O(3)-C(3)	126.8(7)
W-O(4)-C(4)	138.0(7)	W-N(5)-C(51)	174.1(7)

Symmetry operation for primed atoms: $1 - x, 1 - y, 1 - z$.

Table 2 Atomic coordinates for complex 10

Atom	x	y	z
W	0.428 12(4)	0.422 32(3)	0.406 67(3)
O(1)	0.398 9(7)	0.448 7(6)	0.540 0(5)
C(1)	0.260 8(14)	0.442 9(13)	0.581 3(9)
O(2)	0.564 6(6)	0.286 7(6)	0.443 6(5)
C(2)	0.541 3(13)	0.167 2(11)	0.485 2(9)
O(3)	0.516 3(9)	0.427 3(6)	0.296 9(5)
C(3)	0.553 2(14)	0.315 4(12)	0.243 3(8)
O(4)	0.326 9(8)	0.583 9(6)	0.385 6(5)
C(4)	0.181 0(12)	0.627 4(13)	0.373 8(10)
N(5)	0.280 0(8)	0.315 7(7)	0.386 4(6)
C(51)	0.169 1(10)	0.221 7(10)	0.376 2(7)
C(52)	0.030 6(12)	0.249 4(12)	0.403 5(9)
C(53)	-0.080 2(13)	0.157 6(15)	0.392 5(10)
C(54)	-0.053 7(13)	0.033 9(13)	0.354 5(9)
C(55)	0.086 8(12)	0.008 3(11)	0.326 5(9)
C(56)	0.197 7(13)	0.100 9(11)	0.336 2(9)
C(57)	-0.172 6(22)	-0.071 7(16)	0.347 8(14)

Solid-state Structures of $[W(NC_6H_4Me-4)(OMe)_4]$ **10**, $[W(NC_6H_4Me-4)(OPr^i)_4]$ **11** and $[W(NC_6H_4Me-4)(OC_6H_{11})_5Li_2Cl(C_6H_{11}OH)]_2 \cdot C_6H_{11}OH$ **13**.—As expected, the binuclear imidoalkoxide compounds **10** and **11** adopt centrosymmetric distorted edge-shared bioctahedral geometries analogous to the phenylimido compound **1** and the oxoalkoxides $[WO(OMe)_4]$ and $[WO(OC_6H_{11})_4]$. The structures are shown in Figs. 1 and 2 with relevant bond distances and angles in Tables 1 and 3 and atomic coordinates in Tables 2 and 4 respectively.

The short $W \equiv N$ distances and the large WNC angles are

Table 3 Selected bond lengths (Å) and angles (°) for complex 11

W-O(1)	2.029(4)	W-O(2)	1.927(3)
W-O(3)	1.905(4)	W-O(4)	1.914(5)
W-N	1.738(4)	W-O(1')	2.243(3)
O(1)-C(11)	1.461(8)	O(2)-C(21)	1.381(7)
O(3)-C(31)	1.417(8)	O(4)-C(41)	1.364(11)
N-C(51)	1.397(6)		
O(1)-W-O(2)	89.8(1)	O(1)-W-O(3)	91.9(2)
O(2)-W-O(3)	164.0(2)	O(1)-W-O(4)	159.3(1)
O(2)-W-O(4)	84.1(2)	O(3)-W-O(4)	88.7(2)
O(1)-W-N	99.8(2)	O(2)-W-N	98.2(2)
O(3)-W-N	97.1(2)	O(4)-W-N	100.7(2)
O(1)-W-O(1')	69.9(1)	O(2)-W-O(1')	83.9(1)
O(3)-W-O(1')	81.8(1)	O(4)-W-O(1')	89.8(1)
N-W-O(1')	169.5(2)	W-O(1)-C(11)	130.0(3)
W-O(1)-W'	110.1(1)	C(11)-O(1)-W'	119.7(3)
W-O(2)-C(21)	132.1(3)	W-O(3)-C(31)	138.3(5)
W-O(4)-C(41)	137.4(4)	W-N-C(51)	177.4(4)

Symmetry operation for primed atoms: $1 - x, 1 - y, 1 - z$.

Table 4 Atomic coordinates for complex 11

Atom	x	y	z
W	0.460 17(2)	0.575 88(2)	0.631 32(2)
O(1)	0.378 2(3)	0.502 4(3)	0.521 0(2)
C(11)	0.243 2(6)	0.485 0(6)	0.531 5(5)
C(12)	0.107 8(6)	0.629 2(7)	0.529 7(7)
C(13)	0.244 1(8)	0.385 5(7)	0.620 9(6)
O(2)	0.577 8(4)	0.376 4(3)	0.679 2(3)
C(21)	0.616 4(7)	0.317 6(6)	0.780 7(5)
C(22)	0.569 6(9)	0.201 8(8)	0.808 8(7)
C(23)	0.786 7(9)	0.255 0(9)	0.782 7(8)
O(3)	0.395 2(4)	0.761 1(4)	0.560 1(3)
C(31)	0.264 3(12)	0.900 4(8)	0.561 8(7)
C(32)	0.277 4(25)	0.996 2(12)	0.621 1(16)
C(33)	0.240 0(20)	0.964 7(11)	0.460 2(9)
O(4)	0.599 7(4)	0.612 1(4)	0.697 8(3)
C(41)	0.597 2(8)	0.723 9(9)	0.753 8(6)
C(42)	0.755 2(9)	0.701 7(10)	0.750 0(7)
C(43)	0.522 1(10)	0.748 2(12)	0.864 0(7)
N	0.312 4(4)	0.633 2(4)	0.735 3(3)
C(51)	0.198 4(5)	0.676 1(5)	0.822 2(4)
C(52)	0.205 1(7)	0.581 8(7)	0.902 8(5)
C(53)	0.089 9(8)	0.621 3(8)	0.989 3(6)
C(54)	-0.031 1(7)	0.757 0(8)	0.996 3(5)
C(55)	-0.034 9(7)	0.850 6(7)	0.915 7(6)
C(56)	0.078 6(7)	0.813 5(7)	0.829 9(6)
C(57)	-0.157 6(9)	0.800 3(10)	1.090 7(7)

similar to those we have observed in other tungsten *p*-tolylimido compounds^{9,11} and also to those in structurally characterised phenylimido alkoxides^{5,6,12} [except for **1** for which a rather imprecise value of 1.61(4) Å was reported]. We can therefore assign a W-N bond order of close to three and address the question of whether, and to what extent, the W-N bond order is reduced from three by competitive W-OR π bonding. Assuming for the moment that this would be reflected in the structural parameters of the imido ligand, then variation of the ligand set in octahedral complexes of the type $[W(NR)L_4L']$ might be expected to provide structural evidence for such competition for metal π orbitals. We have now structurally characterised a range of *p*-tolylimidochloro and alkoxo complexes and the W-N bond lengths and WNC angles are collected in Table 5 for comparison. Alkoxides are generally regarded as better π donors than chloro ligands, so greater π donation from the alkoxo ligands might be expected to result in longer W-N distances and smaller WNC angles. Although the bond lengths in Table 5 might at first appear to follow this trend, the differences are small and are not likely to be significant given the standard deviations.

If we now turn our attention to the alkoxide ligands, it is

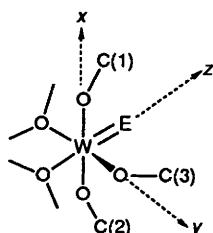
Table 5 Tungsten–nitrogen distances and WNC angles in *p*-tolylimido tungsten complexes

Compound	W–N/Å	WNC/°	Ref.
[{W(NC ₆ H ₄ Me-4)Cl ₄ } ₂]	1.712(18)	177.3(15)	9
[P(CH ₂ Ph)Ph ₃][W(NC ₆ H ₄ Me-4)Cl ₅]	1.741(4)	170.8(5)	11a
	1.709(11)	173.5(12)	11b
[W(NC ₆ H ₄ Me-4)Cl ₄ (thf)]	1.711(7)	177.4(4)	11a
10 [W(NC ₆ H ₄ Me-4)(OMe) ₄]	1.749(8)	174.1(7)	This work
11 [W(NC ₆ H ₄ Me-4)(OPr ⁱ) ₄]	1.738(4)	177.4(4)	This work
13 [W(NC ₆ H ₄ Me-4)(OC ₆ H ₁₁) ₅ Li ₂ Cl(C ₆ H ₁₁ OH)] ₂ ·C ₆ H ₁₁ OH	1.746(6)	175.6(5)	This work

Table 6 Torsion angles E≡W–O–C in dimeric alkoxides [{W(E)(OR)₄}₂]

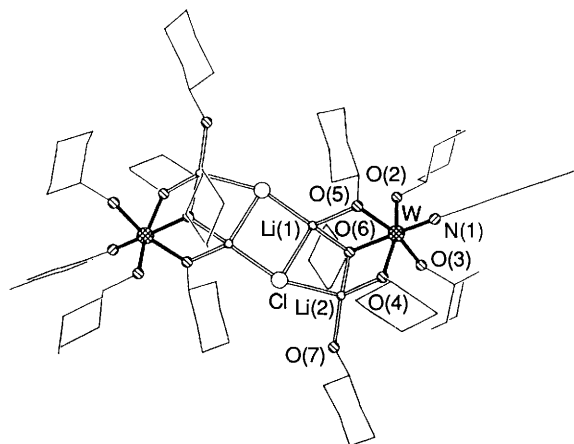
Compound	E	R	Torsion angle/°		
			to C(1)	to C(2)	to C(3)
8	O	Me	–163.9	152.2	53.5
			–162.8	152.2	54.2
9	O	C ₆ H ₁₁	–42.1	–42.1	–67.7
10	NC ₆ H ₄ Me-4	Me	11.5	–30.3	–48.9
11	NC ₆ H ₄ Me-4	Pr ⁱ	–44.0	–12.8	–47.9

possible that their orientation and W–O bond lengths might reveal any W–OR π bonding. We have calculated the O≡W–O–C torsion angles in tungsten oxoalkoxides, [WO(OR)₄],⁴ and in Table 6 these are combined with the analogous N≡W–O–C torsion angles for **10** and **11**. Using a labelling scheme as shown in the diagram below, values of 0 or 180° are optimum for π interaction with d_{xy} while $\pm 90^\circ$ is ideal for interaction with d_{xz} or d_{yz} orbitals. On inspection of Table 6 it can be seen that in each of the imidoalkoxides **10** and **11** one of the *trans* axial alkoxy ligands is oriented to enable preferential π interaction with the d_{xy} orbital. This is also the case for the oxomethoxide **8**, but in the oxocyclohexoxide **9**, perhaps for



steric reasons, it is the equatorial, terminal alkoxy group which is best oriented for π interaction with the metal (*via* the d_{xy} orbital).

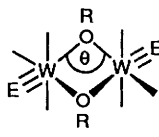
We are therefore unable to reach any firm conclusions regarding the relative degrees of W–E π bonding in these oxo and organoimido compounds by considering the bond lengths and orientations of the terminal ligands. However, the NMR studies discussed in the next section demonstrate that the substitution of an organoimido group for an oxo ligand does have a significant effect on the lability of this type of binuclear complex. We were therefore interested to see if the different *trans* effects of oxo and organoimido ligands might be reflected in the bond lengths and angles around the alkoxy bridges. Table 7 shows a collection of parameters for the bridging region of the oxo- and organoimido-alkoxides. The longer W–O bond *trans* to the oxo or imido ligand is the one most likely to break in any solution dynamic process. We shall discuss the comparative solution behaviour of these molecules in the next section, but point out here that the imidomethoxide **10** has the shortest W–O_{*trans*} and the longest W–O_{*cis*} bond lengths, whereas the imidoisopropoxide **11** has similar bridging dimensions to the oxomethoxide **8**. In fact, if we define Δ as the difference between W–O_{*trans*} and W–O_{*cis*} to reflect the strength of the bridging

**Fig. 3** A view of the molecular structure of complex **13**. In this Figure and in Fig. 4, organic groups are represented by line drawings for clarity

interactions (where a larger Δ implies a more labile dimer), then Δ is the same (0.21 Å) for all except the imidomethoxide **10** (0.11 Å). These results show that the bridging interactions in these compounds are determined by a combination of the *trans* influence of the strongly π -bonding ligand (E) and the steric requirements of the bridging alkoxide. For the less bulky methoxides, the greater *trans* influence of the oxo ligand results in a longer W–O_{*trans*} in **8**, whereas in the secondary alkoxides steric effects become significant, resulting in similar bridging W–O distances for **9** and **11**. On this basis, we would expect **10** to be the least dynamic of these compounds in solution, and this is borne out by our NMR studies.

The stronger *trans* influence of the oxo ligand in **8** compared with the *p*-tolylimido ligand in **10** is in accord with previous expectations where the order of *trans* influence has been given as nitrido > oxo > imido,³ but it should be noted that in the crystal structure of the compound [W(NBu^t)(O)Cl₂(bipy)] (bipy = 2,2'-bipyridine)¹³ the W–N_{bipy} bond *trans* to NBU^t is 0.022 Å longer than that *trans* to the oxo ligand. This is probably due to the inductive effect of the Bu^t group and serves to illustrate the electronic flexibility of the NR group in coordination chemistry.

We were keen to obtain the crystal structure of the cyclohexoxo derivative **12** for a direct comparison with the oxo analogue **9**, but our efforts to prepare **12** by treating [W(NC₆H₄Me-4)Cl₄] with LiOC₆H₁₁ resulted instead in the formation of the mixed-metal alkoxide **13**. A view of the molecule is shown in Fig. 3 and bond distances and angles and atomic coordinates are given in Tables 8 and 9. This dimeric species can be viewed as resulting from the incorporation of LiCl into the notional heterometallic imidoalkoxide [W(NC₆H₄Me-4)(OC₆H₁₁)₅Li(C₆H₁₁OH)] and is structurally analogous to the previously reported¹⁴ oxoisopropoxide of rhenium [{ReO(OPrⁱ)₅Li₂Cl(thf)₂}]₂·2thf **15** shown in Fig. 4. A recent review¹⁵ reflects the increasing interest in heterometallic alkoxides, and the structure of a related halide-free sodium tungsten oxoethoxide [{WO(OEt)₅Na(EtOH)₂}]₂ **16** has also been described.¹⁶ The trinuclear MM'₂ cores present in these

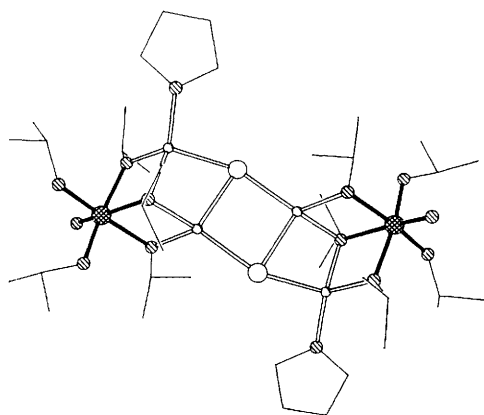
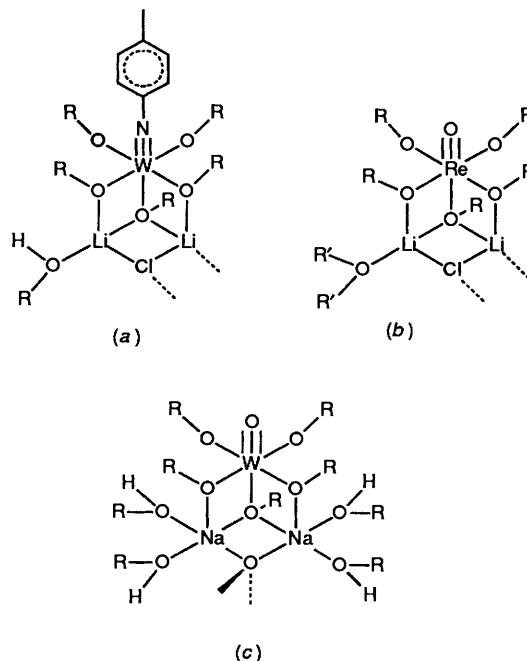
Table 7 Bridging parameters in dimeric alkoxides [$\{W(E)(OR)_4\}_2$]


Compound	E	R	W-O _{cis} /Å	W-O _{trans} /Å	Δ	θ/°	W-W/Å	Ref.
8	O	Me	2.029(7)	2.254(7)	0.21 (av.)	110.3(2)	3.517	4
			2.035(6)	2.230(6)		111.0(2)	3.518	
9	O	C ₆ H ₁₁	2.044(4)	2.250(4)	0.21	110.9(2)	3.539	4
10	NC ₆ H ₄ Me-4	Me	2.072(7)	2.181(6)	0.11	108.5(3)	3.453	This work
11	NC ₆ H ₄ Me-4	Pr ⁱ	2.029(4)	2.243(3)	0.21	110.1(1)	3.504	This work

Table 8 Selected bond lengths (Å) and angles (°) for complex 13

W-N(1)	1.746(6)	W-O(2)	1.912(5)
W-O(3)	1.904(4)	W-O(4)	2.005(5)
W-O(5)	1.976(4)	W-O(6)	2.097(4)
N(1)-C(11)	1.403(9)	O(2)-C(21)	1.428(8)
O(3)-C(31)	1.442(9)	O(4)-C(41)	1.431(10)
O(4)-Li(2)	1.926(12)	O(5)-C(51)	1.431(7)
O(5)-Li(1)	1.978(13)	O(6)-C(61)	1.451(9)
O(6)-Li(1)	1.981(12)	O(6)-Li(2)	1.988(14)
Cl-Li(1)	2.439(13)	Cl-Li(2)	2.417(12)
Cl-Li(1')	2.327(14)	Li(2)-O(7)	1.962(12)
O(7)-C(71)	1.446(10)		
N(1)-W-O(2)	99.4(2)	N(1)-W-O(3)	97.8(2)
O(2)-W-O(3)	90.3(2)	N(1)-W-O(4)	97.0(2)
O(2)-W-O(4)	163.5(2)	O(3)-W-O(4)	88.6(2)
N(1)-W-O(5)	97.8(2)	O(2)-W-O(5)	90.5(2)
O(3)-W-O(5)	164.1(2)	O(4)-W-O(5)	86.2(2)
N(1)-W-O(6)	174.2(2)	O(2)-W-O(6)	85.5(2)
O(3)-W-O(6)	85.3(2)	O(4)-W-O(6)	78.1(2)
O(5)-W-O(6)	78.9(2)	W-N(1)-C(11)	175.6(5)
W-O(2)-C(21)	128.6(5)	W-O(3)-C(31)	132.5(5)
W-O(4)-C(41)	124.1(3)	W-O(4)-Li(2)	102.1(5)
C(41)-O(4)-Li(2)	128.3(5)	W-O(5)-C(51)	131.5(4)
W-O(5)-Li(1)	101.8(4)	C(51)-O(5)-Li(1)	126.0(5)
W-O(6)-C(61)	122.3(3)	W-O(6)-Li(1)	97.5(4)
C(61)-O(6)-Li(1)	122.2(6)	W-O(6)-Li(2)	96.9(4)
C(61)-O(6)-Li(2)	120.8(4)	Li(1)-O(6)-Li(2)	89.6(5)
Li(1)-Cl-Li(2)	70.3(4)	Li(1)-Cl-Li(1')	82.7(4)
Li(2)-Cl-Li(1')	146.5(5)	O(5)-Li(1)-O(6)	81.7(5)
O(5)-Li(1)-Cl	122.5(7)	O(6)-Li(1)-Cl	95.7(5)
O(5)-Li(1)-Cl'	122.6(5)	O(6)-Li(1)-Cl'	137.8(7)
Cl-Li(1)-Cl'	97.3(4)	O(4)-Li(2)-O(6)	82.6(5)
O(4)-Li(2)-Cl	117.0(5)	O(6)-Li(2)-Cl	96.2(5)
O(4)-Li(2)-O(7)	119.9(8)	O(6)-Li(2)-O(7)	143.2(7)
Cl-Li(2)-O(7)	97.7(5)	Li(2)-O(7)-C(71)	137.3(6)

Symmetry operation for primed atoms: 1 - x, 1 - y, -z.

**Fig. 4** A view of the molecular structure of [$\{ReO(OPr^i)_5Li_2Cl(thf)\}_2$] drawn using coordinates from ref. 14

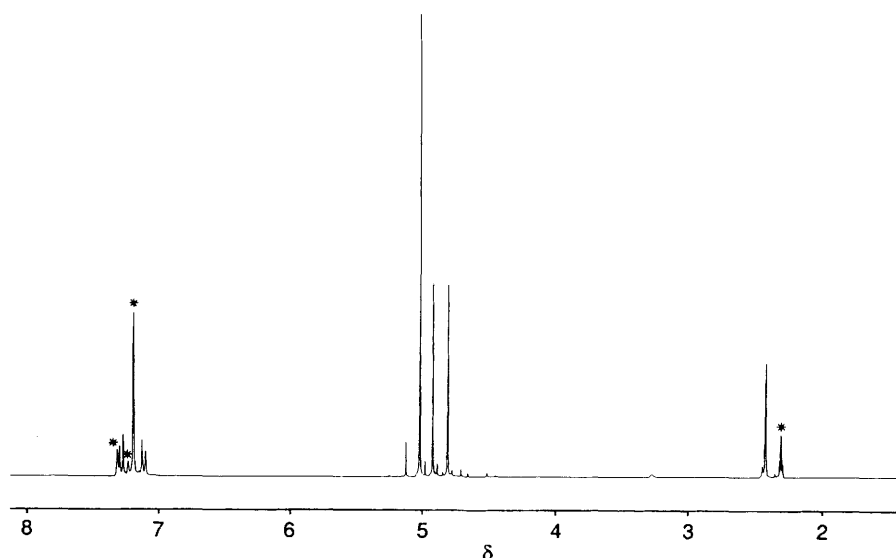
compounds are represented diagrammatically above by (a), (b) and (c) and it is readily apparent that a considerable variation in metal and ligand set can be tolerated by this basic structural unit. The structural parameters in the MO_6 octahedra ($M = W$ or Re) are very similar, and in all three cases the W-O bond lengths *trans* to E ($E = NC_6H_4Me$ or O) are somewhat shorter than in the binuclear compounds discussed above or in the thf adduct [$W(NC_6H_4Me-4)Cl_4(thf)$] [2.237(6) Å].^{11a} The reason for the lack of any significant *trans* influence from the multiply bonded terminal ligands in this type of heterometallic structure is not obvious. The presence of an extra non-co-ordinated disordered alcohol in 13 can be rationalised by hydrogen bonding between O(7) and O(8) (O...O distance 2.720 Å), but in the rhenium isopropoxide 16 this type of interaction is not present and the extra thf molecules are simply occupying space in the lattice as solvent molecules of crystallisation.

Solution ¹H NMR Studies of Organoimidoalkoxides [$W(NC_6H_4Me-4)(OR)_4$].—We invariably found the initial products from the attempted preparations of these alkoxides to be mixtures of compounds, as has previously been noted for the phenylimido compound 1.⁵ In most cases, however, careful recrystallisation provided samples of single compounds which were sufficiently pure for ¹H NMR investigations.

The ¹H NMR spectrum of the methoxide 10 is shown in Fig. 5. The methoxide region contains a well resolved 2:1:1 pattern (in addition to a few minor impurity peaks) consistent with the

Table 9 Atomic coordinates for complex **13**

Atom	x	y	z	Atom	x	y	z
W	0.563 94(3)	0.383 04(2)	0.251 04(2)	C(46)	0.665 8(7)	0.676 5(6)	0.152 4(4)
N(1)	0.685 5(5)	0.334 7(5)	0.303 3(3)	O(5)	0.655 1(4)	0.362 5(4)	0.148 5(2)
C(11)	0.777 1(6)	0.294 1(5)	0.350 2(4)	C(51)	0.775 7(6)	0.297 9(6)	0.125 1(4)
C(12)	0.881 3(7)	0.326 3(7)	0.330 0(5)	C(52)	0.776 1(7)	0.191 7(6)	0.098 0(5)
C(13)	0.971 6(7)	0.284 1(7)	0.375 8(5)	C(53)	0.900 2(9)	0.125 6(8)	0.064 6(6)
C(14)	0.964 4(7)	0.211 1(7)	0.442 9(4)	C(54)	0.955 3(8)	0.198 6(9)	0.001 6(6)
C(15)	0.859 8(8)	0.182 1(7)	0.462 8(4)	C(55)	0.957 0(8)	0.303 5(9)	0.028 7(6)
C(16)	0.767 6(7)	0.221 3(6)	0.417 6(4)	C(56)	0.830 8(7)	0.369 7(7)	0.061 5(5)
C(17)	1.063 4(8)	0.168 9(9)	0.491 1(6)	O(6)	0.426 5(3)	0.452 8(3)	0.181 5(2)
O(2)	0.528 6(4)	0.243 7(4)	0.257 3(2)	C(61)	0.314 2(5)	0.425 8(6)	0.199 6(4)
C(21)	0.533 2(6)	0.154 9(6)	0.320 5(4)	C(62)	0.311 7(7)	0.343 3(7)	0.149 6(5)
C(22)	0.427 2(7)	0.113 2(7)	0.326 2(5)	C(63)	0.191 8(8)	0.318 5(8)	0.165 9(6)
C(23)	0.429 8(8)	0.019 1(7)	0.394 3(5)	C(64)	0.090 4(8)	0.428 0(9)	0.153 7(6)
C(24)	0.544 6(9)	-0.078 0(7)	0.385 3(6)	C(65)	0.092 7(7)	0.515 0(8)	0.200 8(6)
C(25)	0.653 4(8)	-0.035 9(7)	0.375 6(5)	C(66)	0.213 5(6)	0.535 5(7)	0.186 0(5)
C(26)	0.648 5(7)	0.058 2(6)	0.308 9(4)	Cl	0.472 2(2)	0.634 8(2)	0.030 3(1)
O(3)	0.441 0(4)	0.425 9(4)	0.333 6(2)	Li(1)	0.527 8(10)	0.433 5(11)	0.081 5(7)
C(31)	0.441 3(7)	0.458 8(7)	0.406 3(4)	Li(2)	0.428 9(10)	0.612 5(10)	0.168 3(7)
C(32)	0.403 2(8)	0.374 3(8)	0.469 9(4)	O(7)	0.327 3(5)	0.768 4(5)	0.178 1(4)
C(33)	0.276 7(10)	0.376 5(10)	0.469 6(6)	C(71)	0.230 7(7)	0.825 5(7)	0.231 9(5)
C(34)	0.188 8(9)	0.496 0(11)	0.474 9(7)	C(72)	0.115 4(8)	0.863 1(7)	0.199 5(6)
C(35)	0.225 0(9)	0.578 9(9)	0.409 6(6)	C(73)	0.014 9(9)	0.924 3(9)	0.254 3(6)
C(36)	0.355 1(8)	0.574 3(7)	0.410 9(5)	C(74)	0.039 3(9)	1.021 9(9)	0.277 6(7)
O(4)	0.563 4(4)	0.545 3(3)	0.225 3(2)	C(75)	0.156 1(9)	0.985 5(11)	0.307 1(6)
C(41)	0.666 8(6)	0.581 6(6)	0.220 7(4)	C(76)	0.259 3(8)	0.922 3(9)	0.252 0(6)
C(42)	0.665 0(6)	0.624 7(6)	0.294 4(4)	O(8)	0.379 4(14)	0.891 2(11)	0.041 8(8)
C(43)	0.773 3(8)	0.668 7(8)	0.289 4(5)	C(81)	0.380 0(12)	0.991 6(9)	-0.009 7(8)
C(44)	0.777 5(8)	0.758 7(8)	0.220 8(6)	C(82)	0.394 2(12)	1.074 6(9)	0.037 8(7)
C(45)	0.774 0(7)	0.718 4(7)	0.147 0(5)	C(83)	0.511 7(13)	1.037 5(10)	0.067 5(7)

**Fig. 5** 300 MHz ^1H NMR spectrum of complex **10** in $[\text{}^2\text{H}_8]$ toluene. Solvent peaks are indicated by asterisks

solid-state structure shown in Fig. 1. These lines did not broaden appreciably when the temperature of the sample was raised to 350 K, indicating that the bridging bonds in **10** are much less labile than those in the oxomethoxide **8** for which we have observed coalescence in the ^1H NMR spectrum at around 325 K.

Although there was no evidence for site exchange with increasing temperature, a spin-polarisation transfer experiment with inversion of the central methoxide resonance (Fig. 6) demonstrated that there is slow exchange between all three sites in solution. One other interesting feature of this experiment was the observation of a positive nuclear Overhauser effect (NOE) for the aromatic doublet at δ 7.3. Using the crystal-structure determination to estimate the closest approach between the

ortho hydrogens of the imido group and the hydrogens of the methoxides in the bridging plane (assuming normal C-H bond lengths and allowing free rotation about W-N, N-C, W-O and C-O bonds to bring the relevant atoms as close together as possible) an assignment of the central peak to the terminal methoxide (closest approach *ca.* 1.70 Å) rather than the bridging methoxide (closest approach *ca.* 1.95 Å) is possible.

At 305 K the ^1H NMR spectrum of **11** shows the slightly broadened methyl and methine resonances of only one isopropoxide environment in addition to associated methyl and aromatic peaks of the imido group and some minor impurity peaks [Fig. 7(a)]. The bulkier isopropoxide **11** is therefore much more dynamic than the methoxide **10**. The results of a variable-temperature ^1H NMR study are shown in Fig. 7 and these

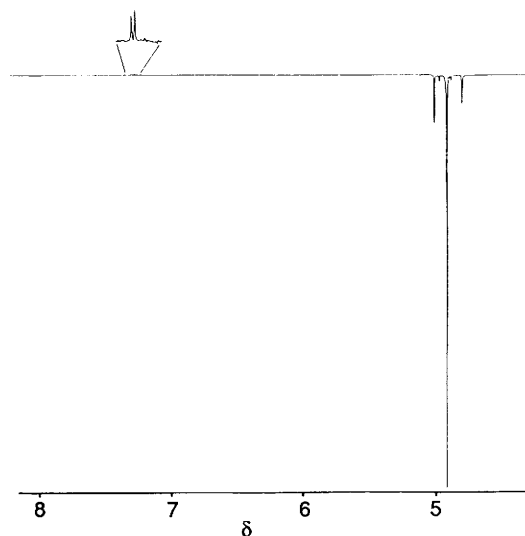


Fig. 6 300 MHz ^1H polarisation-transfer NMR spectrum of complex **10** with inversion of the central methoxide peak

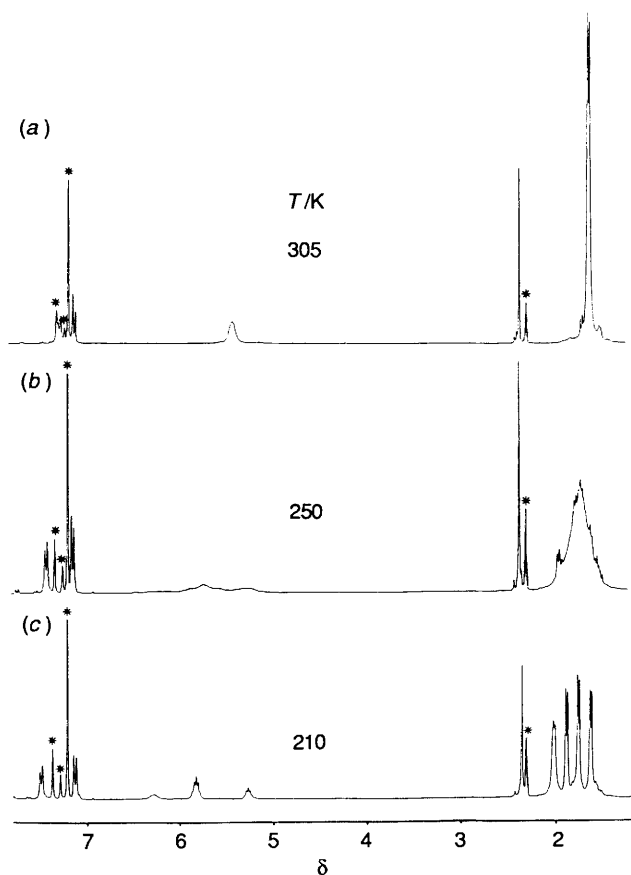
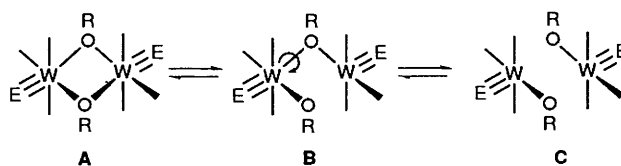


Fig. 7 Variable-temperature 300 MHz ^1H NMR spectra of complex **11** in $[\text{2H}_8]\text{toluene}$. Solvent peaks are indicated by asterisks

suggest that an intramolecular redistribution of the type proposed for the oxomethoxide **8**⁴ rather than a monomer/dimer equilibrium is responsible for this dynamic behaviour. Hence, the spectrum of the dimeric solid-state structure is frozen out at 210 K (the presence of four doublets in the high-field region confirming the diastereotopic nature of the CH_3 groups in the *trans*-axial OPr^i ligands) and as the temperature is raised the isopropoxide peaks gradually broaden and then coalesce. We could see no evidence for the appearance and growth with



increasing temperature of peaks due to a mononuclear compound.

If we represent the bond-breaking process involved in the dynamics of these binuclear alkoxides $[\{\text{W}(\text{E})(\text{OR})_4\}_2]$ by A–C above, we can begin to rationalise the subtle interplay of factors affecting the differences in solution behaviour of the various compounds. In the oxomethoxide **8** the first bridging bond breaks fairly readily to give **B** ($\text{E} = \text{O}$; $\text{R} = \text{Me}$) and the methoxide ligands do not restrict the rotation indicated which results in alkoxide site exchange. Because of the weaker *trans* effect of the arylimido ligand, the bridging bonds in **10** are stronger and the compound is much less dynamic in solution than **8**. The introduction of bulkier alkoxides causes steric compression, and in the oxoisopropoxide $[\text{WO}(\text{OPr}^i)_4]$ this makes further $\text{W}-\text{O}$ bond dissociation to give **C** more favourable than rotation of the $\text{WO}(\text{OPr}^i)_4$ fragments in **B**. Hence, **A** and **C** ($\text{E} = \text{O}$; $\text{R} = \text{Pr}^i$) are observed in equilibrium in the ^1H NMR spectrum of this compound.⁴ In the arylimidoisopropoxide **11**, steric effects again facilitate the formation of **B** but, because of the weaker *trans* effect of the imido group, rotation can still occur before the second bond dissociation, and intramolecular site exchange in **A** ($\text{E} = \text{NC}_6\text{H}_4\text{Me}$; $\text{R} = \text{Pr}^i$) is observed in the ^1H NMR spectrum. The approximate ΔG^\ddagger values for alkoxide site exchange in **8** and **11** are 68 and 54 kJ mol^{-1} respectively at coalescence.

The ^1H and ^{13}C chemical shifts of the NCH_2 methylene group in $[\{\text{W}(\text{NBu}^n)(\text{OMe})_4\}_2]$ are respectively 1.03 and 7.33 ppm upfield of those in $[\{\text{W}(\text{NBu}^n)\text{Cl}_4\}_2]$. This presumably reflects a shift in electron density onto nitrogen with the greater π donation to tungsten from the alkoxide ligands. Variable-temperature ^1H NMR spectroscopy of $[\{\text{W}(\text{NBu}^n)(\text{OMe})_4\}_2]$ indicates very slow site exchange, hence the *n*-butylimido group has a similar *trans* effect to the *p*-tolylimido ligand. However, from our observation that the *tert*-butylimido group can exert a stronger *trans* influence than an oxo ligand¹³ we would expect $[\text{W}(\text{NBu}^i)(\text{OR})_4]$ compounds to be more labile than their oxo or arylimido analogues discussed above. In this regard, it is interesting that Bradley *et al.*⁸ have proposed a monomeric, trigonal-bipyramidal structure of $[\text{W}(\text{NBu}^i)(\text{OPr}^i)_4]$ based on its ^1H NMR spectrum, which showed the presence of two types of isopropoxide in the ratio of 3:1. This is consistent with the general picture of solution dynamics outlined above.

In our attempts to obtain the cyclohexoxide **12** we tried treating $[\text{W}(\text{NC}_6\text{H}_4\text{Me-4})\text{Cl}_4]$ with cyclohexanol and *tert*-butylamine, although Nielson *et al.*⁵ had shown that a similar reaction involving $\text{W}(\text{NPh})\text{Cl}_4$, Pr^iOH and Bu^iNH_2 produced the amine adduct $[\text{W}(\text{NPh})(\text{OPr}^i)_4(\text{Bu}^i\text{NH}_2)]$. It was evident from microanalysis results and from ^1H NMR and IR spectra that our product was impure and contained some Bu^iNH_2 . The ^1H NMR spectrum contains well separated methyl and aromatic resonances for two *p*-tolylimido groups in addition to broad cyclohexyl resonances between δ 4.2 and 5.2 (methine hydrogens) and between δ 1.2 and 2.2 (ring methylenes). A sharp Bu^i peak is present at δ 1.22 and a broad peak at δ 3.75 is possibly due to NH_2 . This suggests that a mixture of approximately equal amounts of **12** and the amine adduct $[\text{W}(\text{NC}_6\text{H}_4\text{Me-4})(\text{OC}_6\text{H}_{11})_4(\text{Bu}^i\text{NH}_2)]$ has been produced.

Crystal Structure of $[\text{NBu}^n_4][\text{W}_2(\text{NPh})_2(\text{OMe})\text{Cl}_6]$.—In an attempt to prepare a mixed oxidation-state polynuclear organo-imido compound, the phenylimidomethoxide **1** was treated with the tetra-*n*-butylammonium salt of the binuclear tungsten(v)

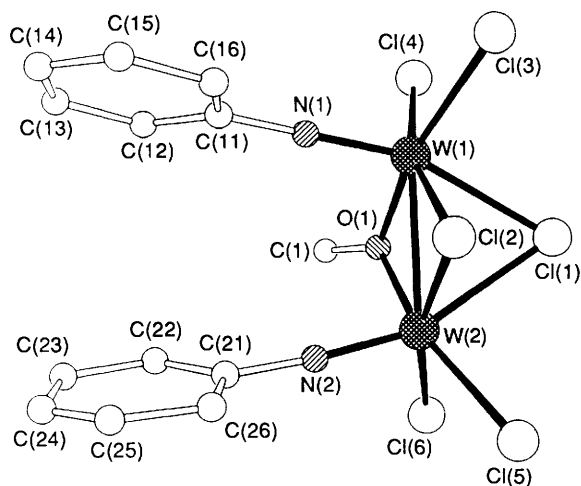


Fig. 8 A view of the molecular structure of $[W_2(NPh)_2(OMe)Cl_6]^-$

Table 10 Selected bond lengths (Å) and angles (°) for complex 17

W(1)–W(2)	2.695(1)	W(1)–Cl(1)	2.627(3)
W(1)–Cl(2)	2.421(4)	W(1)–Cl(3)	2.386(2)
W(1)–Cl(4)	2.376(3)	W(1)–O(1)	2.024(5)
W(1)–N(1)	1.705(7)	W(2)–Cl(1)	2.632(3)
W(2)–Cl(2)	2.423(3)	W(2)–Cl(5)	2.362(3)
W(2)–Cl(6)	2.361(2)	W(2)–O(1)	2.002(5)
W(2)–N(2)	1.722(7)	O(1)–C(1)	1.355(13)
N(1)–C(11)	1.429(10)	N(2)–C(21)	1.416(12)
W(2)–W(1)–Cl(1)	59.2(1)	W(2)–W(1)–Cl(2)	56.2(1)
Cl(1)–W(1)–Cl(2)	76.3(1)	W(2)–W(1)–Cl(3)	133.9(1)
Cl(1)–W(1)–Cl(3)	92.7(1)	Cl(2)–W(1)–Cl(3)	83.5(1)
W(2)–W(1)–Cl(4)	127.7(1)	Cl(1)–W(1)–Cl(4)	92.7(1)
Cl(2)–W(1)–Cl(4)	163.9(1)	Cl(3)–W(1)–Cl(4)	85.5(1)
W(2)–W(1)–O(1)	47.6(1)	Cl(1)–W(1)–O(1)	72.5(1)
Cl(2)–W(1)–O(1)	103.5(2)	Cl(3)–W(1)–O(1)	161.2(2)
Cl(4)–W(1)–O(1)	83.7(2)	W(2)–W(1)–N(1)	101.9(2)
Cl(1)–W(1)–N(1)	160.9(2)	Cl(2)–W(1)–N(1)	90.8(2)
Cl(3)–W(1)–N(1)	99.8(2)	Cl(4)–W(1)–N(1)	102.5(2)
O(1)–W(1)–N(1)	97.5(2)	W(1)–W(2)–Cl(1)	59.1(1)
W(1)–W(2)–Cl(2)	56.2(1)	Cl(1)–W(2)–Cl(2)	76.2(1)
W(1)–W(2)–Cl(5)	133.2(1)	Cl(1)–W(2)–Cl(5)	91.1(1)
Cl(2)–W(2)–Cl(5)	83.7(1)	W(1)–W(2)–Cl(6)	128.1(1)
Cl(1)–W(2)–Cl(6)	94.1(1)	Cl(2)–W(2)–Cl(6)	165.2(1)
Cl(5)–W(2)–Cl(6)	85.4(1)	W(1)–W(2)–O(1)	48.3(1)
Cl(1)–W(2)–O(1)	72.7(2)	Cl(2)–W(2)–O(1)	104.1(2)
Cl(5)–W(2)–O(1)	159.3(2)	Cl(6)–W(2)–O(1)	83.1(2)
W(1)–W(2)–N(2)	101.6(2)	Cl(1)–W(2)–N(2)	160.4(2)
Cl(2)–W(2)–N(2)	90.7(2)	Cl(5)–W(2)–N(2)	102.0(2)
Cl(6)–W(2)–N(2)	101.3(2)	O(1)–W(2)–N(2)	97.1(3)
W(1)–Cl(1)–W(2)	61.7(1)	W(1)–Cl(2)–W(2)	67.6(1)
W(1)–O(1)–W(2)	84.1(2)	W(1)–O(1)–C(1)	134.3(6)
W(2)–O(1)–C(1)	135.2(7)	W(1)–N(1)–C(11)	170.9(5)
W(2)–N(2)–C(21)	173.7(5)		

anion¹⁷ $[W_2(NPh)_2Cl_7]^-$. An X-ray crystal structure analysis of the red prisms obtained from dichloromethane–hexane showed that ligand exchange had resulted in substitution of one of the bridging chlorides in the W^V starting material by a methoxide. The anion of $[NBu^4][W_2(NPh)_2(OMe)Cl_6]$ **17** is shown in Fig. 8 and bond distances and angles are given in Table 10 with atomic coordinates in Table 11. Presumably the other product is $[W(NPh)(OMe)_3Cl_2]$ which remains in solution.

This anion is one of a family of confacial-bioctahedral tungsten(v) complexes and has the same gross structural features as the chloro derivatives $[W_2(E)_2(\mu-Cl)_3Cl_4]^-$ ($E = O, N^iEt$ or NPh).¹⁷ Again, the *trans* influence of the organoimido ligand is evident, the *trans* W–Cl bridging bonds being

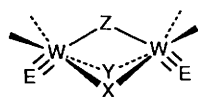
Table 11 Atomic coordinates for complex 17

Atom	x	y	z
W(1)	0.505 56(2)	0.581 50(2)	0.728 01(2)
W(2)	0.687 39(2)	0.510 21(2)	0.729 47(2)
Cl(1)	0.563 3(2)	0.449 0(1)	0.809 5(1)
Cl(2)	0.534 5(2)	0.478 3(2)	0.638 7(2)
Cl(3)	0.334 1(2)	0.534 1(2)	0.694 2(2)
Cl(4)	0.451 8(2)	0.651 5(2)	0.827 1(2)
Cl(5)	0.736 7(2)	0.374 8(2)	0.701 0(2)
Cl(6)	0.830 9(2)	0.505 9(2)	0.827 9(1)
O(1)	0.646 5(4)	0.604 3(3)	0.788 4(3)
C(1)	0.693 5(9)	0.672 4(7)	0.822 9(8)
N(1)	0.503 0(4)	0.658 8(4)	0.664 2(4)
C(11)	0.495 0(5)	0.713 7(4)	0.602 1(4)
C(12)	0.541 6(6)	0.790 1(5)	0.612 0(5)
C(13)	0.529 1(7)	0.844 1(5)	0.552 3(5)
C(14)	0.471 9(10)	0.821 7(7)	0.485 7(6)
C(15)	0.427 9(8)	0.743 8(7)	0.477 3(5)
C(16)	0.438 9(7)	0.689 0(6)	0.535 6(5)
N(2)	0.732 2(5)	0.569 9(4)	0.665 4(4)
C(21)	0.757 8(6)	0.620 2(6)	0.608 6(5)
C(22)	0.789 0(8)	0.699 7(6)	0.623 4(6)
C(23)	0.814 0(10)	0.749 2(9)	0.567 2(8)
C(24)	0.806 1(12)	0.713 0(11)	0.498 6(9)
C(25)	0.770 4(14)	0.638 7(11)	0.483 5(8)
C(26)	0.749 4(10)	0.585 7(8)	0.539 0(6)
N(3)	0.284 1(5)	0.321 0(5)	0.837 4(5)
C(311)	0.350 5(7)	0.309 5(5)	0.781 6(5)
C(312)	0.327 9(6)	0.233 9(8)	0.729 7(8)
C(313)	0.401 3(7)	0.232 1(9)	0.675 7(5)
C(314)	0.508 7(6)	0.209 9(11)	0.717 2(7)
C(321)	0.320 9(8)	0.399 7(7)	0.879 6(6)
C(322)	0.262 9(14)	0.422 0(11)	0.939 7(11)
C(323)	0.284 3(20)	0.512 2(14)	0.966 5(18)
C(324)	0.399 0(22)	0.525 4(21)	0.993 1(19)
C(331)	0.173 3(6)	0.325 9(6)	0.799 8(5)
C(332)	0.146 6(6)	0.398 0(7)	0.745 8(7)
C(333)	0.031 8(7)	0.406 6(8)	0.719 0(7)
C(334)	0.007 0(11)	0.482 7(10)	0.668 2(11)
C(341)	0.292 0(6)	0.245 8(8)	0.889 6(7)
C(342)	0.400 4(6)	0.226 1(11)	0.931 1(7)
C(343)	0.398 9(13)	0.150 2(10)	0.982 4(6)
C(344)	0.360 5(32)	0.177 7(15)	1.052 0(12)

considerably longer than those *cis* to NPh . The methoxide is *cis* to both imido ligands, facilitating any π interactions with metal orbitals not used for π bonding to the imido groups. The structural effects of introducing a bridging methoxide can be appreciated by considering the bond lengths and angles in Table 12. The W–OMe bond distances are slightly smaller than the shorter bridging bond lengths in the $[W(E)(OR)_4]_2$ dimers ($E = O$ or NR) discussed earlier, and are typical of μ -OR distances observed in a range of lower oxidation-state molybdenum and tungsten alkoxides.¹⁸ Since these distances are shorter than the W–Cl bridging bonds, the core of the molecule contracts slightly resulting in smaller W–Cl–W bridging angles and a shorter W–W distance in the methoxide **17**.

All of these anions are diamagnetic and the question arises as to whether a direct metal–metal bond is present. Although the W–W distance of 2.695 Å compares with the distances observed in d^1 – d^1 compounds containing $M_2(\mu-OR)_2$ ($M = Mo$ or W) where single bonds have been assigned,¹⁸ a theoretical analysis of the various factors which might determine molecular geometry in M_2L_9 complexes¹⁹ concluded that in only a minority of examples is direct metal–metal bonding important, and that a delocalised bonding scheme involving orbitals from the bridging ligands is more appropriate.

In solution, both 1H and ^{13}C NMR spectra of **17** contain two methoxide resonances in CD_3CN and CD_2Cl_2 respectively. The difference in the chemical shifts of these peaks suggests that a mixture of isomers is present with the methoxide in either terminal or bridging positions.

Table 12 Selected bond lengths (Å) and angles (°) in confacial bioctahedral tungsten(v) oxo and organoimido anions

Anion	W-E	W-W	W-X	W-Y	W-Z	WXW	WYW	WZW	XWY	XWZ	YWZ
[W ₂ O ₂ Cl ₇] ⁻ *	1.67	2.849	2.434	2.420	2.606	71.7	72.1	66.3	106.8	76.0	77.0
[W ₂ (NEt) ₂ Cl ₇] ⁻ *	1.69	2.839	2.432	2.416	2.585	71.0	71.6	66.8	106.7	78.1	77.3
[W ₂ (NPh) ₂ Cl ₇] ⁻ *	1.72	2.835	2.423	2.440	2.575	71.6	71.8	66.6	106.7	76.8	77.1
17 [W ₂ (NPh) ₂ (OMe)Cl ₆] ⁻	1.71	2.695	2.422 (Cl)	2.013 (OMe)	2.630	67.6	84.1	61.7	103.8	76.3	72.6

* Ref. 17.

Experimental

All manipulations were carried out under dry, oxygen-free conditions using standard Schlenk techniques, or in a dry-box fitted with a recirculation system. Hydrocarbon, thf and Et₂O solvents were dried over and distilled from sodium-benzophenone immediately prior to use. Methanol was distilled over magnesium methoxide. Propan-2-ol and cyclohexanol were distilled from the corresponding sodium alkoxides and stored over 4 Å molecular sieves, and Bu^tOH was used as its benzene azeotrope. Infrared spectra were recorded as Nujol mulls between CsI plates on a Perkin Elmer 598 spectrometer and NMR spectra were recorded on Bruker WP 200 or WM 300 spectrometers. Elemental analyses were performed by the microanalytical service, the University of Newcastle upon Tyne.

Preparations.—[W(NC₆H₄Me-4)(OMe)₄] **10**. Methanol (1.0 cm³, 25.3 mmol) and *tert*-butylamine (2.5 cm³, 23.8 mmol) were added to [W(NC₆H₄Me-4)Cl₄]^o (2.28 g, 5.3 mmol) suspended in benzene (25 cm³). The mixture was stirred for 24 h, filtered and the solvent removed *in vacuo*. The resulting gum was extracted with hot hexane (25 cm³) and after removal of the solvent, the residue was recrystallised from acetonitrile to give golden prisms (0.92 g, 42%) (Found: C, 31.0; H, 4.4; N, 3.5. C₁₁H₁₉NO₄W requires C, 32.3; H, 4.5; N, 4.0%). IR: 1598w, 1564w, 1503m, 1362s, 1218w, 1172w, 1155m, 1105m, 1075s, 1050s, 1030m, 1019m, 1006m, 829s, 728w, 702w, 587s, 558w, 540s, 520s (br), 473m, 444m, 349w, 341m, 300w and 238w cm⁻¹; δ_H(300.14 MHz, C₆D₅CD₃) 7.29, 7.27, 7.12, 7.10 (4 H, NC₆H₄Me), 5.01 [6 H, s, (OCH₃)₂], 4.91 (3 H, s, OCH₃), 4.80 (3 H, s, OCH₃) and 2.42 (3 H, s, NC₆H₄CH₃); δ_C(50.32 MHz, CD₃CN) 167.47, 137.52, 128.61, 127.67 (NC₆H₄Me), 64.21, 62.26, 62.09 (OCH₃) and 19.94 (NC₆H₄CH₃).

[W(NC₆H₄Me-4)(OPrⁱ)₄] **11**. Lithium isopropoxide (1.73 g, 6.2 mmol) was added to a solution of [W(NC₆H₄Me-4)Cl₄] in thf (40 cm³) at -70 °C and the mixture was allowed to warm to room temperature. Volatiles were removed after stirring for 15 h and, after extraction with ether and solvent removal, the residue was recrystallised from acetonitrile (35 cm³) to give golden prisms (1.35 g, 42%) (Found: C, 42.4; H, 6.8; N, 2.7. C₁₀H₃₅NO₄W requires C, 43.4; H, 6.9; N, 2.7%). IR: 1598w, 1584w, 1560w, 1500m, 1325m, 1168m, 1125s, 1020w, 975s (br), 844m, 822m, 728w, 622w, 600m, 567w and 472w cm⁻¹; δ_H(300.14 MHz, C₆D₅CD₃) 7.31, 7.29, 7.15, 7.12 (4 H, NC₆H₄Me), 5.48 (4 H, br s, OCHMe₂) and 2.37 (3 H, s, NC₆H₄CH₃); δ_C(50.32 MHz, CD₃CN) 146.00, 129.50, 128.49, 114.75 (NC₆H₄Me), 76.01 (OCHMe₂), 25.63 (NC₆H₄CH₃) and 24.67 [OCH(CH₃)₂].

[W(NC₆H₄Me-4)(OC₆H₁₁)₄] **12**. Cyclohexanol (1.57 cm³, 15.1 mmol) and *tert*-butylamine (1.59 cm³, 15.1 mmol) were added to [W(NC₆H₄Me-4)Cl₄] (1.63 g, 3.8 mmol) in hexane (30 cm³) and the mixture was stirred for 24 h. The solution was filtered and cooled to -25 °C to give a yellow crystalline product (0.6 g) which is probably a mixture of **12** and [W(NC₆H₄Me-4)(OC₆H₁₁)₄(NH₂Bu^t)] (Found: C, 54.1; H,

7.5; N, 2.9. C₆₆H₁₁₃N₃O₄W₂ requires C, 54.9; H, 7.9; N, 2.9%). IR: 3330w, 3270w, 1620w, 1563m, 1498m, 1316m, 1268m, 1252m, 1220m, 1181w, 1149w, 1130m, 1067s (br), 1020s, 975s (br), 927m, 913w, 890m, 865w, 848s, 819s, 791m, 752w, 702w, 667s (br), 625m, 555 (sh), 548m, 535m, 514m, 498w, 462m, 458m, 433w, 409m, 380m, 312m, 300m and 275m cm⁻¹; δ_H(300.14 MHz, CD₂Cl₂) 7.15, 7.12, 6.95, 6.92 (8 H, NC₆H₄Me), 4.25–5.05 (8 H, br m, OCH), 3.75 (2 H, br, NH₂), 2.44 (3 H, s, NC₆H₄CH₃), 2.21 (3 H, s, NC₆H₄CH₃), 2.02, 1.99, 1.71, 1.46, 1.29 (80 H, br m, CH₂) and 1.22 [9 H, s, H₂NC(CH₃)₃]; δ_C(75.47 MHz, CD₂Cl₂) 136.00, 130.30, 129.16, 127.58, 116.80 (NC₆H₄Me), 83.72 (br, OCH), 50.40 (H₂NCMe₃), 36.56 (br, CH₂), 31.99 [C(CH₃)₃], 26.8 (NC₆H₄CH₃) and 25.06 (br, CH₂).

[{W(NC₆H₄Me-4)(OC₆H₁₁)₅LiCl(C₆H₁₁OH)₂}]₂·C₆H₁₁OH **13**. Lithium cyclohexoxide (0.97 g, 9.15 mmol) was added to a solution of [W(NC₆H₄Me-4)Cl₄] (0.98 g, 2.28 mmol) in thf (40 cm³) at 0 °C. The resulting yellow solution was stirred for 24 h, filtered and the solvent removed under reduced pressure to give a yellow solid (1.41 g, 68%). Crystals suitable for X-ray diffraction were obtained from toluene-hexane at -25 °C (Found: C, 52.9; H, 8.0; N, 1.4. C₄₉H₈₆ClLi₂NO₇W requires C, 52.9; H, 7.5; N, 1.5%). IR: 3480m, 1500m, 1319w, 1307w, 1268m, 1150w, 1131m, 1092m, 1070s, 1036s, 994s, 980s, 931w, 894m, 852m, 846m, 821s, 792m, 741m, 716m, 688m, 667s, 648m, 628s, 540m, 520s, 470m, 439m and 390w cm⁻¹; δ_H(300.14 MHz, CD₃CN) 7.31, 7.29, 7.14, 7.11, 6.97, 6.94, 6.61, 6.58 (NC₆H₄Me), 5.2–3.8 (br m, OCH), 3.52 (m, CHOH), 2.64 [d, ³J(HH) 4.3 Hz, CHOH], 2.23 (s, NC₆H₄CH₃), 1.87, 1.77, 1.60 and 1.28 (multiplets, CH₂).

[W(NC₆H₄Me-4)(OBu^t)₄] **14**. A solution of lithium *tert*-butoxide (1.46 g, 18.2 mmol) in ether (20 cm³) was added to [W(NC₆H₄Me-4)Cl₄] (1.96 g, 4.55 mmol) in ether (30 cm³) and the mixture was stirred for 15 h. After filtration, removal of the solvent from the filtrate gave a yellow solid (0.66 g). This was shown to contain several products by ¹H NMR, but recrystallisation from acetonitrile gave a single compound. IR: 1493w, 1352s, 1231w (br), 1166s (br), 1020w, 967m, 938s, 903w, 813m (br), 660w, 635w, 549w (br) and 470w cm⁻¹; δ_H(200.13 MHz, CD₃CN) 7.17, 7.15, 6.60, 6.58 (4 H, NC₆H₄Me), 2.42 (3 H, s, NC₆H₄CH₃) and 1.48 [36 H, s, OC(CH₃)₃].

[W(NBuⁿ)Cl₄]. A mixture of WCl₄ (1.55 g, 4.55 mmol) and BuⁿNCO (0.52 cm³, 4.55 mmol) in octane (70 cm³) was heated under reflux for 15 h. The resulting brownish solution was cooled to -25 °C to deposit an orange solid which was filtered off, washed with hexane and dried *in vacuo* (1.57 g, 87%) (Found: C, 12.6; H, 2.3; N, 3.5. C₄H₉Cl₄NW requires C, 12.1; H, 2.3; N, 3.5%). δ_H(300.14 MHz, C₆D₆) 6.02 [2 H, t, ³J(HH) 6.3 Hz, NCH₂], 1.45 (2 H, m, NCH₂CH₂), 1.25 [2 H, m, N(CH₂)₂CH₂] and 0.72 [3 H, t, ³J(HH) 7.3 Hz, N(CH₂)₃CH₃]; δ_C(75.47 MHz, C₆D₆) 68.38 (NCH₂), 33.19 (NCH₂CH₂), 21.38 [N(CH₂)₂CH₂] and 13.98 [N(CH₂)₃CH₃].

[{W(NBuⁿ)(OMe)₄}]₂. Methanol (0.52 cm³, 12.8 mmol) was added to a solution of [W(NBuⁿ)Cl₄] (1.27 g, 3.2 mmol) in thf

Table 13 Crystallographic data

Compound	10	11	13	17
Formula	C ₂₂ H ₃₈ N ₂ O ₈ W ₂	C ₃₈ H ₇₀ N ₂ O ₈ W ₂	C ₉₂ H ₁₆₀ Cl ₂ Li ₄ N ₂ O ₁₃ W ₂	C ₂₉ H ₄₉ Cl ₆ N ₃ OW ₂
<i>M</i>	826.3	1050.7	1968.7	1036.1
Crystal system	Monoclinic	Triclinic	Triclinic	Monoclinic
Space group	<i>P</i> 2 ₁ / <i>c</i>	<i>P</i> $\bar{1}$	<i>P</i> $\bar{1}$	<i>P</i> 2 ₁ / <i>n</i>
<i>a</i> /Å	9.1611(8)	10.197(2)	11.908(5)	13.448(6)
<i>b</i> /Å	10.1018(6)	10.333(2)	12.582(5)	16.057(7)
<i>c</i> /Å	15.2007(10)	12.339(3)	17.940(8)	18.394(7)
α /°	90	87.08(1)	79.12(2)	90
β /°	92.483(6)	83.05(2)	79.54(3)	101.82(5)
γ /°	90	61.36(1)	71.00(3)	90
<i>U</i> /Å ³	1405.4	1132.6	2474.8	3887.7
<i>Z</i>	2	1	1	4
<i>D</i> _c /cm ⁻³	1.952	1.540	1.321	1.770
μ /mm ⁻¹	8.40	5.23	2.48	6.48
<i>F</i> (000)	792	524	1024	2008
Crystal size/mm	0.12 × 0.25 × 0.35	0.46 × 0.54 × 0.62	0.30 × 0.60 × 0.80	0.40 × 0.40 × 0.60
Transmission factors	0.050–0.158	0.148–0.225	0.177–0.242	0.031–0.068
2θ _{max} /°	50	50	45	50
Reflections measured	2524	6500	7076	10 379
Unique reflections	2464	3981	6423	6814
Observed reflections	2037	3650	5626	5060
<i>R</i> _{int}	0.032	0.032	0.042	0.020
No. of refined parameters	155	227	527	371
<i>R</i>	0.0476	0.0273	0.0393	0.0427
<i>R</i> ' = ($\Sigma w\Delta^2/\Sigma wF_o^2$) ^{1/2}	0.0577	0.0297	0.0375	0.0351
Goodness of fit	1.59	1.99	2.03	1.43
Mean, max. shift/e.s.d.	0.009, 0.060	0.021, 0.216	0.003, 0.009	0.036, 0.420
Max., min. electron density/e Å ⁻³	1.86, -2.19	1.24, -0.58	1.24, -1.53	1.15, -0.91

(40 cm³). Ammonia was immediately bubbled through the solution for 5 min, and the mixture was then stirred for 16 h. The suspension was filtered and solvent removed *in vacuo* to give a yellow glassy solid (0.27 g, 60%) (Found: C, 24.6; H, 5.6; N, 3.7. C₈H₂₁NO₄W requires C, 25.6; H, 5.6; N, 3.7%). IR: 1300s, 1260m, 1160m, 1105m, 1075s, 1020m (br), 952m, 918w, 895w, 802m, 728s, 568m (br) and 510m cm⁻¹; δ _H(300.14 MHz, C₆D₅CD₃) 4.99 [2 H, t, ³*J*(HH) 4.6, NCH₂], 4.86 (6 H, OCH₃), 4.83 (3 H, OCH₃), 4.66 (3 H, OCH₃), 1.67 (2 H, m, NCH₂CH₂), 1.60 [2 H, m, N(CH₂)₂CH₂] and 1.03 [3 H, t, ³*J*(HH) 7.2 Hz, N(CH₂)₃CH₃]; δ _C(50.32 MHz, C₆D₅CD₃) 65.35 (OCH₃), 63.29 (OCH₃), 62.70 [(OCH₃)₂], 61.05 [NCH₂, ³*J*(CW) 15 Hz], 36.70 (NCH₂CH₂), 21.50 [N(CH₂)₂CH₂] and 14.77 [N(CH₂)₃CH₃].

[NBuⁿ₄][W₂(NPh)₂(OMe)Cl₆] **17**. The compound [W-(NPh)(OMe)₄] (0.45 g, 1.13 mmol) was added to a solution of [NBuⁿ₄][W₂(NPh)₂Cl₇] (1.17 g, 1.12 mmol) in CH₂Cl₂ (15 cm³). After 12 h a hexane layer was added and orange-red prisms were produced over the course of several days (0.79 g, 68%) (Found: C, 33.6; H, 4.8; N, 4.0. C₂₉H₄₉Cl₆N₃OW₂ requires C, 35.1; H, 4.7; N, 4.0%). IR: 1580w, 1565w, 1174w, 1159w, 1075m, 1061m, 1050m, 1031s, 995m, 895w, 881w, 775m, 766s, 741m, 729m, 691m, 627w, 558w, 546m, 472w, 390m, 347m, 329s, 301m, 280w and 249w cm⁻¹; δ _H(300.14 MHz, CD₃CN) 7.8–6.7 (10 H, series of complex multiplets, NC₆H₅), 5.05 (s) and 4.89 (s) (3 H, OCH₃), 3.09 (8 H, m, NCH₂), 1.61 (8 H, m, NCH₂CH₂), 1.35 [8 H, m, N(CH₂)₂CH₂] and 0.99 [12 H, t, (CH₂)₃CH₃]; δ _C(50.32 MHz, CD₃CN) 154.70, 128.08, 128.00, 127.84, 126.89, 125.92 (NC₆H₅), 68.59, 65.17 (OCH₃), 59.31 (NCH₂), 24.34 (NCH₂CH₂), 19.97 [N(CH₂)₂CH₂] and 13.94 [N(CH₂)₃CH₃].

X-Ray Crystallography.—Data were measured at room temperature on a Stoe-Siemens diffractometer with graphite-monochromated Mo-K α radiation ($\lambda = 0.71073$ Å), from crystals sealed in Lindemann capillaries. Crystallographic data are summarised in Table 13. Cell parameters were refined in each case from 2θ values of 32 reflections (20–25°) measured with ω - θ scans; on-line profile fitting was used for **17**.²⁰ Corrections were made for intensity decay and for absorption (semiempirically). Atoms were located from Patterson and

difference syntheses and refined anisotropically by blocked-cascade least-squares methods²¹ on *F* for reflections with $F > 4\sigma(F)$; weighting was of the form $w = 1/\sigma^2(F)$, with contributions from both counting statistics and an analysis of variance.²² Hydrogen atoms were included in calculated positions for **11** (except methyl groups), **13** (except OH groups) and **17**, with isotropic thermal parameters. The cation bond lengths and angles for **17** were restrained, as the atoms appeared to be somewhat disordered. The unco-ordinated cyclohexanol molecule in **13** lies on a centre of symmetry, so the OH group is disordered over two sites on opposite sides of the ring, each within hydrogen-bonding distance of the OH group of a cyclohexanol molecule co-ordinated to lithium. An isotropic extinction parameter *x* was refined to $2.4(6) \times 10^{-7}$ for **13**, such that $F_c' = F_c/(1 + xF_c^2/\sin 2\theta)^{1/2}$; extinction effects were insignificant for the other structures. Atomic scattering factors were taken from ref. 23.

Additional material available from the Cambridge Crystallographic Data Centre comprises H-atom coordinates, thermal parameters and remaining bond lengths and angles.

Acknowledgements

We thank the SERC for financial support and for an Earmarked Studentship (to C. R.). We are also grateful to Dr. M. N. S. Hill for his assistance with NMR experiments.

References

- R. R. Schrock, J. S. Murdzek, G. Bazan, J. Robbins, M. DiMare and M. O'Regan, *J. Am. Chem. Soc.*, 1990, **112**, 3875.
- J. D. Buntington and R. K. Grasselli, *J. Catal.*, 1979, **59**, 79.
- W. A. Nugent and J. M. Mayer, *Metal-Ligand Multiple Bonds*, Wiley, New York, 1988.
- W. Clegg, R. J. Errington, P. Kraxner and C. Redshaw, *J. Chem. Soc., Dalton Trans.*, 1992, 1431.
- A. J. Nielson, J. M. Waters and D. C. Bradley, *Polyhedron*, 1985, **4**, 285.
- P. A. Bates, A. J. Nielson and J. M. Waters, *Polyhedron*, 1987, **6**, 163.
- S. F. Pedersen and R. R. Schrock, *J. Am. Chem. Soc.*, 1982, **104**, 7483.
- D. C. Bradley, A. J. Howes, M. B. Hursthouse and J. D. Runnacles, *Polyhedron*, 1991, **10**, 477.

- 9 W. Clegg, R. J. Errington and C. Redshaw, *Acta Crystallogr., Sect. C*, 1987, **43**, 2223.
- 10 D. C. Bradley, M. H. Chisholm, M. W. Extine and M. E. Stager, *Inorg. Chem.*, 1977, **16**, 1794.
- 11 (a) D. C. Bradley, R. J. Errington, M. B. Hursthouse, R. L. Short, B. R. Ashcroft, G. R. Clark, A. J. Nielson and C. E. F. Rickard, *J. Chem. Soc., Dalton Trans.*, 1987, 2067; (b) W. Clegg, R. J. Errington and C. Redshaw, *Acta Crystallogr., Sect. C*, 1989, **45**, 164.
- 12 F. A. Cotton and E. S. Shamsoum, *J. Am. Chem. Soc.*, 1984, **106**, 3222.
- 13 W. Clegg, R. J. Errington, D. C. R. Hockless and C. Redshaw, unpublished work.
- 14 P. G. Edwards, G. Wilkinson, M. B. Hursthouse and K. M. A. Malik, *J. Chem. Soc., Dalton Trans.*, 1980, 2467.
- 15 K. G. Caulton and L. G. Hubert-Pfalzgraf, *Chem. Rev.*, 1990, **90**, 969.
- 16 N. Y. Turova, V. G. Kessler and S. I. Kucheiko, *Polyhedron*, 1991, **10**, 2617.
- 17 D. C. Bradley, R. J. Errington, M. B. Hursthouse and R. L. Short, *J. Chem. Soc., Dalton Trans.*, 1990, 1043.
- 18 M. H. Chisholm, *Polyhedron*, 1983, **2**, 681.
- 19 R. H. Summerville and R. Hoffmann, *J. Am. Chem. Soc.*, 1979, **101**, 3821.
- 20 W. Clegg, *Acta Crystallogr., Sect. A*, 1981, **37**, 22.
- 21 G. M. Sheldrick, SHELXTL, an integrated system for solving, refining and displaying crystal structures from diffraction data, Revision 5, University of Göttingen, 1985.
- 22 Wang Hong and B. E. Robertson, in *Structures and Statistics in Crystallography*, ed. A. J. C. Wilson, Adenine Press, New York, 1985, pp. 125–136.
- 23 *International Tables for X-Ray Crystallography*, Kynoch Press, Birmingham, 1974, vol. 4, pp. 99, 149.

Received 26th June 1992; Paper 2/03367D